Computation of Torque of an Electrical Machine With Different Types of Finite Element Mesh in the Air Gap

Bishal Silwal[1], Paavo Rasilo[1], Lauri Perkkiö[2], Miika Oksman[2], Antti Hannukainen[2], Timo Eirola[2], and Antero Arkkio[1]

[1]Department of Electrical Engineering and Automation, Aalto University, Espoo 02150, Finland
[2]Department of Mathematics and Systems Analysis, Aalto University, Espoo 02150, Finland

In the numerical analysis of electrical machines, accurate computation of the electromagnetic torque is desired. Maxwell stress tensor method and Coulomb's method are the most commonly used methods for computing torque numerically. However, several other methods have also been developed and are being used. These methods are observed to have several accuracy issues related to the finite element discretization used in the air gap of the machine. In this paper, the effect of various finite element meshes in the air gap of the machine and the effect of the shape of the elements used to compute the torque are studied and discussed. This paper carefully compares the torques obtained from a direct method and a method based on the power balance of the machine.

Index Terms—**Electromagnetic torque, energy balance, finite element method, induction machine, mesh.**

I. Introduction

FINITE element method has been a very important tool for the design and analysis of electrical machines. Due to the advancement in the computing technology, it is gaining immense popularity among the developers and researchers all around the world. Torque computation is one of the key issues in the numerical analysis of electrical machines. Maxwell stress tensor method [1] is typically used in finite element analysis to calculate the torque. Coulomb's method based on the principle of virtual work [2] is also commonly used for this purpose. Abdel-Razek *et al.* [3] proposed a method based on the concept of a single element in the uniform part of the air gap of the electric machine, often referred to as air-gap element or macro-element, and claimed it to be relatively more accurate. A variant of Maxwell stress tensor method was proposed in [4] where the stress tensor is integrated over a volume in the air gap of the machine comprised by two concentric boundaries. Several other methods for the calculation of torque have also been developed, used, and discussed in the literature, for example, method based on magnetic coenergy [5] and methods based on stored energy [6], [7]. A semianalytical method is presented in [8] in which the field is solved analytically and the numerically solved potential is used as a boundary condition. Popescu *et al.* [9] presents two other methods, one of which is similar to the above described semi-analytical method, while the other is based on the virtual work principle and segregates the average and pulsating torque components. These methods are tested for a brushless PM motor. Comparison between some numerical methods and analytical torque computation methods can also be found in the literatures [10]–[12].

However, accuracy issues for several of these methods have been reported. For instance, [8], [9] describe the possible numerical errors in field calculations resulting in the inaccuracy in torque calculated with Maxwell stress tensor and Coulomb's method and propose different ways to enhance their accuracies. The accuracy of macro-element method is known to be dependent on the quality of the meshes in the stator and rotor [13]. In recent years, a new formulation based on this method has been presented in [14] and is claimed to be computationally efficient and accurate. Yanni and Aliprantis [15] also use the same method to obtain maximum torque, while optimizing the stator tooth shape. The torque calculated from the finite element analysis is desired to be independent on the type of mesh used in the air gap of the machine and shape of the elements used for torque computation but in practice, it is not true.

In this paper, we study the effect of certain variations of the finite element mesh in the air gap of the machine on the computed torque. Maxwell stress and Coulomb's method give almost the same result when the torque is computed from a band confined between two concentric circles. Here, the torque is computed by the Coulomb's method, given by

$$T = \frac{l}{\mu_0} \sum_{e=1}^{N_{\text{eag}}} \int_{\Omega_e} \left[-\mathbf{B}^T \mathbf{G}^{-1} \frac{\partial \mathbf{G}}{\partial \varphi} \mathbf{B} + \frac{1}{2} B^2 \left|\mathbf{G}\right|^{-1} \frac{\partial \left|\mathbf{G}\right|}{\partial \varphi} \right] d\Omega. \tag{1}$$

The energy balance of the machine can also be used to calculate torque, in the case when the speed of the machine is kept constant. This method based on the energy balance of the machine is presented in this paper. Somewhat similar methods based on power and energy balance have been studied in [4] and [16]. To be able to use the energy balance method, it is very important to have a time integration scheme that is energy balanced. For this, the energy should be conserved in each time step. A detailed study of the instantaneous power balance has been presented in [17]. Trapezoidal rule is known to conserve energy if the system under study is magnetically linear [18], [19]. In this paper, we first study the relative error in the energy balance of an electrical machine when the trapezoidal rule and the implicit Euler are used for time

Manuscript received April 17, 2014; revised May 15, 2014; accepted June 23, 2014. Date of publication June 26, 2014; date of current version December 12, 2014. Corresponding author: B. Silwal (e-mail: bishal.silwal@aalto.fi).

Color versions of one or more of the figures in this paper are available online at http://ieeexplore.ieee.org.

Digital Object Identifier 10.1109/TMAG.2014.2333491

discretizations, which is followed by the study of the effect of different finite element mesh in the air gap of the machine on the torque computed from Coulomb's method and the energy balance method.

II. Energy Balance

A. Torque From Energy Balance

This method is based on the principle of energy conservation in electrical machines. The power balance of an electrical machine in motoring mode is given by

$$P_{\text{in}} = P_{\text{loss}} + \frac{\mathrm{d}W_{\text{f}}}{\mathrm{d}t} + T\omega_{\text{m}} \tag{2}$$

where P_{in} is the input power, P_{loss} is the electromagnetic losses, W_{f} is the energy of the electromagnetic field, and $T\omega_{\text{m}}$ is the power transmitted by the torque.

If the angular speed ω_{m} is assumed to be constant, the power balance expression given by (2) can be integrated for a certain period of time Δt to obtain an expression for the average torque of the machine

$$\int_{t_0}^{t_0+\Delta t} T\,\mathrm{d}t = \frac{1}{\omega_{\text{m}}} \int_{t_0}^{t_0+\Delta t} \left(P_{\text{in}} - P_{\text{loss}} - \frac{\mathrm{d}W_{\text{f}}}{\mathrm{d}t}\right) \mathrm{d}t \tag{3}$$

$$T^{\text{a}} = \frac{P_{\text{in}}^{\text{a}} - P_{\text{loss}}^{\text{a}} - \frac{\Delta W_{\text{f}}}{\Delta t}}{\omega_{\text{m}}^{\text{a}}} \tag{4}$$

where the superscript a denotes the average value.

The stator winding has been modeled as a filamentary winding without eddy currents. In this case, the resistive stator losses can be excluded from the power balance and the input power to the machine is calculated using the currents and the flux linkages of the stator phases

$$P_{\text{in}}^{\text{a}} = \frac{\Delta W_{\text{in}}}{\Delta t} = \frac{1}{\Delta t} \sum_{k=1}^{\text{m}} \int_{\psi_{k0}}^{\psi_{k1}} i_k d\psi_k \tag{5}$$

where i_k is the currents of phase k, $\psi_{k\text{i}}$, and $\psi_{k\text{f}}$ are the flux linkages of phase k at the beginning and end of the period Δt. m is the number of phases. P_{loss} is obtained as

$$P_{\text{loss}}^{\text{a}} = \frac{\Delta W_{\text{loss}}}{\Delta t} = \frac{1}{\Delta t} \int_V \int_{t_0}^{t_0+\Delta t} \left(-\mathbf{E} \cdot \frac{\partial \mathbf{A}}{\partial t}\right) \mathrm{d}t\mathrm{d}V \tag{6}$$

$$= \frac{1}{\Delta t} \int_V \int_{t_0}^{t_0+\Delta t} \sigma \left(\frac{\partial \mathbf{A}}{\partial t} - \frac{u}{l}\mathbf{e}_{\text{z}}\right) \cdot \frac{\partial \mathbf{A}}{\partial t} \mathrm{d}t\mathrm{d}V \tag{7}$$

where V is the volume of the solution region, $\mathbf{E}$ is the electric field strength, $\mathbf{A}$ is the magnetic vector potential, σ is the conductivity, u is the electric scalar potential, and l is the length of the machine. The core losses are not included in this paper.

The change in the magnetic field energy W_f over the period of time is calculated from the magnetization curves of the materials and flux densities $\mathbf{B}_0$ and $\mathbf{B}_1$ at the beginning and the end of the period

$$\Delta W_{\text{f}} = \int_V \int_{B_0}^{B_1} \mathbf{H} \cdot d\mathbf{B}\mathrm{d}V. \tag{8}$$

If one is interested in the instantaneous torque, the Δt in (4) can be equal to the length of one time step. For an average torque in the steady state of the machine, the time interval Δt should be chosen to be at least one fundamental period of the machine. The time derivatives are approximated by first order difference ratios and the time integrals in (3)–(7) are summed up time-step by time-step. Over one time step, the input energy and the energy consumed by the resistive loss in the rotor cage are, respectively

$$\Delta W_{\text{in}} = \sum_{n=1}^{m} [\beta i_{n,k+1} + (1-\beta) i_{n,k}](\psi_{n,k+1} - \psi_{n,k}) \tag{9}$$

$$\Delta W_{\text{rt}} = \int_V \sigma \left\{ \begin{bmatrix} \frac{\mathbf{A}_{k+1} - \mathbf{A}_k}{\Delta t} \\ -\frac{1}{l}[\beta u_{k+1} + (1-\beta) u_k]\mathbf{e}_{\text{z}} \end{bmatrix} \cdot (\mathbf{A}_{k+1} - \mathbf{A}_k) \right\} dV \tag{10}$$

where $\beta = 0.5$ for the trapezoidal rule and $\beta = 1$ for the implicit Euler method.

B. Validity of the Energy Balance

It is important to know whether the numerically computed energy balance is valid. In case of electrical machines, this can be done by studying the energy balance of the machine in the locked rotor condition. We consider a 4 pole, 50 Hz, 37 kW cage induction machine. The main parameters of the machine are given in Table I. A time stepping finite element analysis is performed. One period of the fundamental frequency is divided into 600 time steps and second order triangular elements are used in this paper. In the locked rotor case, as the shaft power is zero, we can see if the input power is in good agreement with the resistive losses and the magnetic field energy. The relative error is calculated as

$$\varepsilon = \frac{\left(P_{\text{in}} - P_{\text{loss}} - \frac{\Delta W_{\text{f}}}{\Delta t}\right)^{\text{a}}}{P_{\text{in}}^{\text{a}}}. \tag{11}$$

The trapezoidal rule and the implicit Euler method are both tested for the energy balance. Both linear and nonlinear magnetic properties of the core materials are used for each of the time integration methods. The absolute values of the relative error when the trapezoidal rule is used are shown in Fig. 1 and that when the implicit Euler method is used are shown in Fig. 2. The relative error is shown with respect to the number of time steps per period of the supply frequency. The error in the energy balance is relatively lower when the trapezoidal rule was used in the simulations. In the linear case, the error is very small and does not change significantly if the length of the time step is reduced, however, it has a decreasing trend in the nonlinear case. With higher number of time steps per period, the error in the nonlinear case reduces significantly. In the case when implicit Euler was used, the order of the error for both linear and nonlinear case does not have much difference. However, these are very high compared with the result from the trapezoidal rule. In the time-stepping finite element simulations of an electrical machines, one period of supply frequency is typically divided to around 400–800 time steps. Results show that for this number of time steps, with

TABLE I
TEST MACHINE PARAMETERS

Parameter	Value
Number of poles	4
Connection	Star
Rated Voltage [V]	400
Supply frequency [Hz]	50
Rated Current [A]	70
Rated Torque [Nm]	240
Rated Power [kW]	37

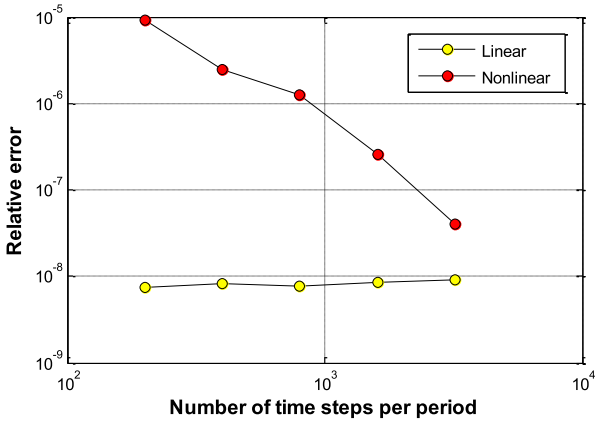

Fig. 1. Relative error in energy balance (trapezoidal rule).

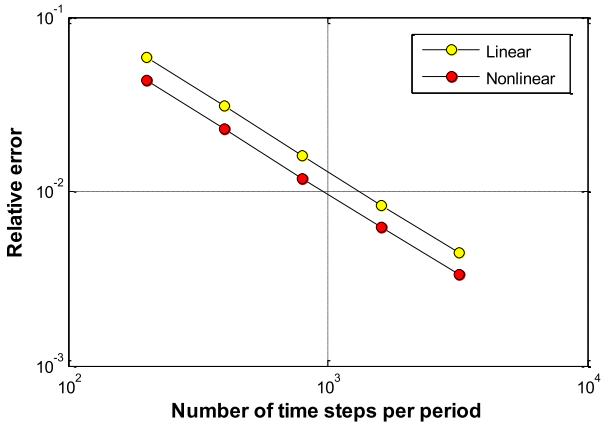

Fig. 2. Relative error in energy balance (implicit Euler).

trapezoidal rule used, the energy balance is well fulfilled to allow torque computation based on it whereas the implicit Euler does not well conserve the energy. In this paper, we use both the time integration methods to see how the torque behaves.

III. METHOD OF ANALYSIS

The effect of various finite element meshes is studied for the torque of a test machine, the main parameters of which are given in Table I. The whole mesh has 4494 elements and 9049 number of nodes. The magnetic field in the core region of the machine is assumed to be 2-D. The 3-D end winding fields are modeled approximately by adding the end-winding impedances to the circuit equations of the windings. For a linear problem, the core of the machine is considered to have a constant relative permeability of 1000 and for a nonlinear problem the nonlinearity is modeled with a single-valued reluctivity curve. The movement of the rotor is taken into consideration by the moving-band technique.

The machine reaches a steady state in a couple of periods of fundamental frequency if the time-stepping simulation is started from a time-harmonic solution as an initial condition. Three periods of 50 Hz frequency are simulated in this paper. The solution of the magnetic field in the cross section of the machine is shown in Fig. 3. Fig. 4 shows four different arrangements of finite element mesh in the air gap consisting of a single, double, and triple layers with two different shapes of elements in the torque computation band.

For a single layer mesh, both the torque computation and the movement of the rotor is done using the same band of elements. But for double and triple layer mesh, the band of elements used for torque computation and the movement of rotor may be same or different. Altogether, 14 different combinations of the number of layers, and the bands used for the torque computation and the rotor movement, as shown in Table II were made. We study the torque for all different mesh combinations and different shapes of the elements used in the computation. The effect of finite element discretization on factors such as harmonics is also presented in brief.

IV. RESULTS

For all 14 combinations, the average torque was calculated. Fig. 5 shows the average torques computed by the Coulomb's method and the energy balance method for a linear case when the trapezoidal rule is used for time integration. The average torque computed from Coulomb's method varies with the variation in the type of mesh and the band used for rotation and torque computation. However, the energy balance method gives average torque that seems to be almost independent on such variations. It is noticeable that when the same band of elements is used both rotation and torque computation (combinations 1, 2, 5, 6, 10, and 14 in Table I), the average torques from both methods are very close. Fig. 6 shows the same for a nonlinear case.

The results from the linear and nonlinear cases when the implicit Euler was used are shown in Figs. 7 and 8, respectively. Even when the implicit Euler is used for time integration, the average torques computed from the Coulomb's method varies with the change in the mesh combinations whereas that computed from the energy balance method is almost constant.

Torque computed from direct methods is dependent not only on the type of the finite element mesh, but also on the shape and the size of the elements used in the torque computation band. For instance, the triangular elements in the middle band of Fig. 4(c) are right-angled. The elements sides in each element can be shifted so that the element gradually becomes a equilateral triangle [Fig. 4(d)]. In this way, the effect of the change in the element shape on the computed torque can be studied.

Ideally, the torque should be independent on the shape of the elements, but results show that the torque computed from the

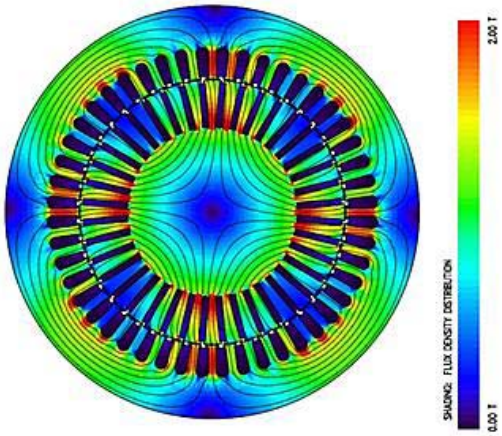

Fig. 3. Field solution of the test machine.

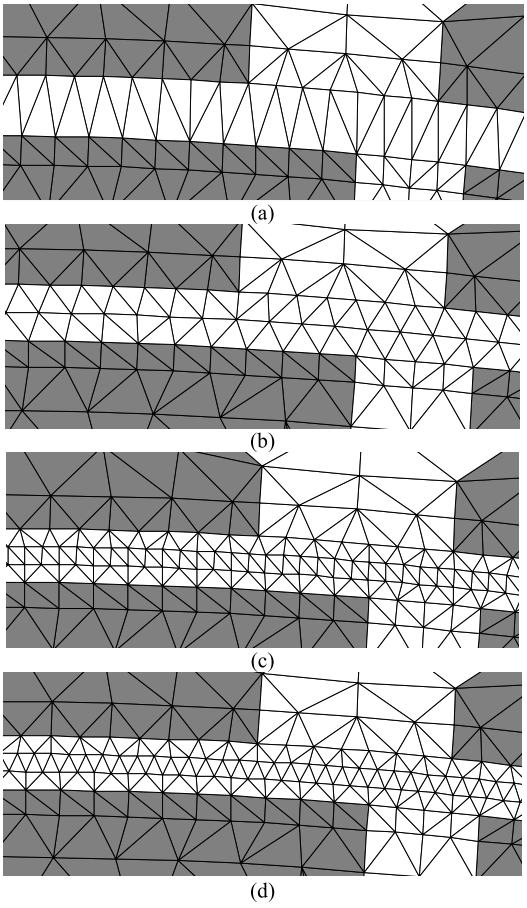

Fig. 4. Finite element mesh in the air gap. (a) One layered. (b) Two layered. (c) Three layered with right-angled triangular elements. (d) Three layered with equilateral triangular elements.

TABLE II
DIFFERENT COMBINATIONS OF LAYERS AND BANDS USED FOR TORQUE COMPUTATION AND ROTOR MOVEMENT

Combination	Number of Bands	Movement Band	Torque Band
1	1	1	1
2	2	1	1
3	2	1	2
4	2	2	1
5	2	2	2
6	3	1	1
7	3	1	2
8	3	1	3
9	3	2	1
10	3	2	2
11	3	2	3
12	3	3	1
13	3	3	2
14	3	3	3

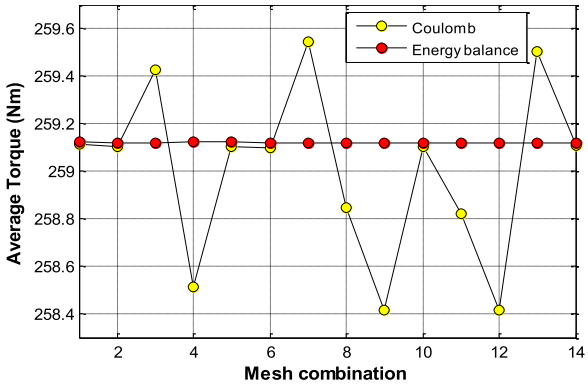

Fig. 5. Average torques for different mesh combinations (linear case and trapezoidal rule).

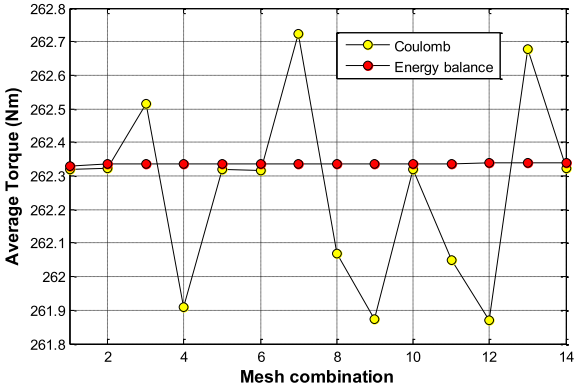

Fig. 6. Average torques for different mesh combinations (nonlinear case and trapezoidal rule).

direct methods vary. For this purpose, a mesh with three layers of elements was used and the middle band was used for torque computation. The elements in this band were shifted gradually from equilateral ones to right-angled ones and back to the equilateral ones. Fig. 9 shows the effect of the change in shape of the elements on the average torque when the trapezoidal rule was used and the problem was linear. Fig. 10 shows the results when the problem was nonlinear. The horizontal axis represents the shift of the element sides scaled by the length of the element side. When the shift is zero, the shape of the elements correspond to right-angled ones and when

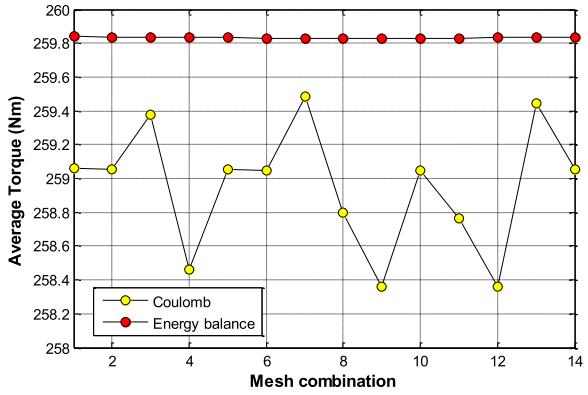

Fig. 7. Average torques for different mesh combinations (linear case and implicit Euler).

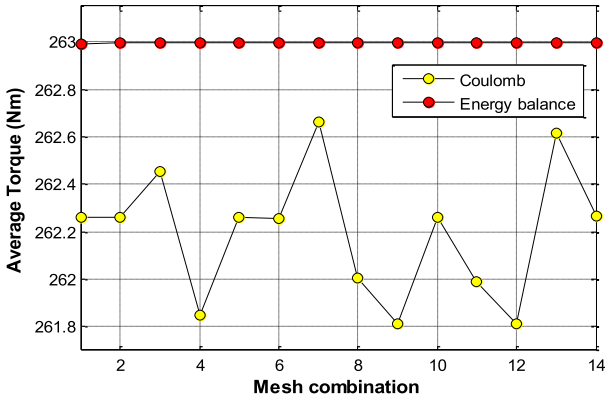

Fig. 8. Average torques for different mesh combinations (nonlinear case and implicit Euler).

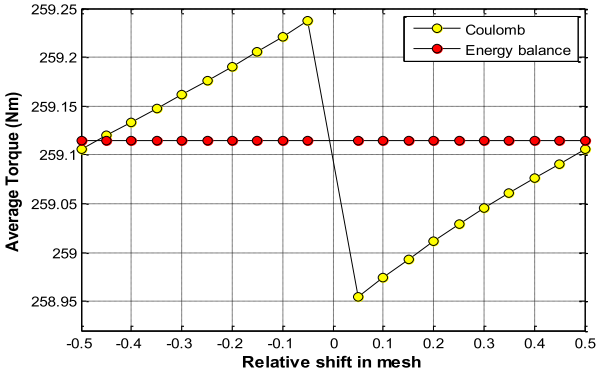

Fig. 9. Effect of the shape of elements in average torques (linear case and trapezoidal rule).

the shift is ± 0.5, the shape of the elements correspond to equilateral ones. The torque from Coulomb's method varies with the change in the element shape. The torque from the energy balance seems to be independent on the shape of the elements. What is interesting here is the typical behavior of the torque when the element shape is changed from the equilateral to the right-angled ones and back to the equilateral again. The average torques calculated from both methods are very close when the elements in the torque computation band are equilateral triangular elements. But the differences increase as the element shape changes to the right-angled ones. The

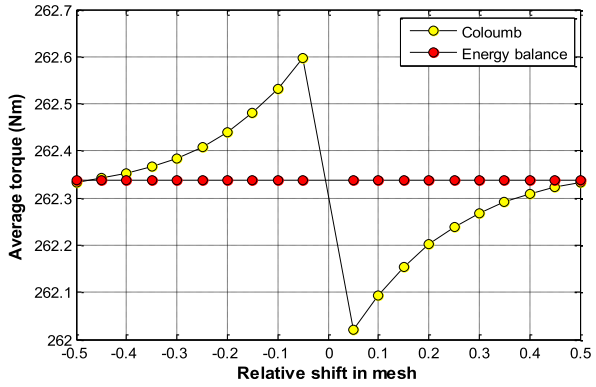

Fig. 10. Effect of the shape of elements in average torque (nonlinear case and trapezoidal rule).

difference between the maximum and the minimum torque, however, is not significantly large. One additional interesting feature in this case is that if an average of the average torques obtained from the Coulomb's method for all different element shapes is calculated, the result is very close to the average torque from energy balance.

For the same mesh, the effect of the element shape was also studied when the implicit Euler method was used for time integration. Figs. 11 and 12 show the results for linear and nonlinear case, respectively. Even in these cases the torques from the Coulomb's method change similarly for different shapes of elements as in the previous case. The energy balance again gives the torque that is insensitive to the change in element shapes. However, for none of the element shapes, the torque from these two methods matches.

Next, the effect of such variation is studied for the case with a two-layered mesh in the air gap. In this case, it is not possible to use a layer of regular elements for torque computation as the number of slots in the stator and the rotor are different. Similar elements shift as was done for three-layered mesh was studied. The results for a linear case using trapezoidal rule are shown in Fig. 13. Here, again the torque computed from Coulomb's method changes with the change in element shapes. But the difference in the torques is relatively larger than that in the earlier case. Again, the torque from the energy balance is seen to be independent from the shape of the elements.

The instantaneous variation of torque is shown in Fig. 14. Since, the energy balance method gives average torques, the instantaneous variation was obtained by setting the period of integration equal to the time step size. This gives the average torques over the time step but the Coulomb's method gives the torque at the end of the time step. This causes a small time shift between the instantaneous torques, which can be observed in the figure. The results shown in Fig. 14 are from the simulation in which the mesh used is a two-layer mesh with the second band used for both rotation and torque computation.

Harmonics are important when the torque of a machine is studied, especially when the machine is provided with a non-sinusoidal supply, for instance, frequency converter supply. However, in this paper, the machine is supplied with sinusoidal voltage. The harmonic components of the torque

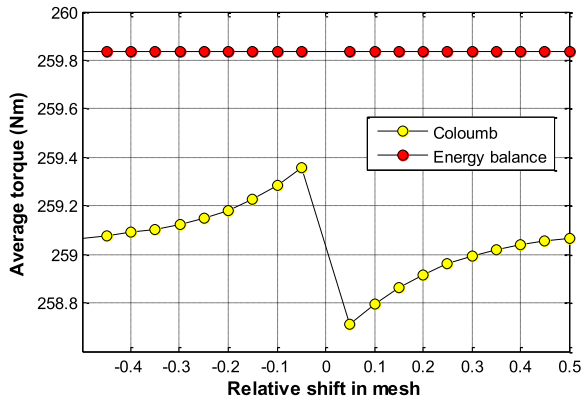

Fig. 11. Effect of the shape of elements in average torque (linear case and implicit Euler).

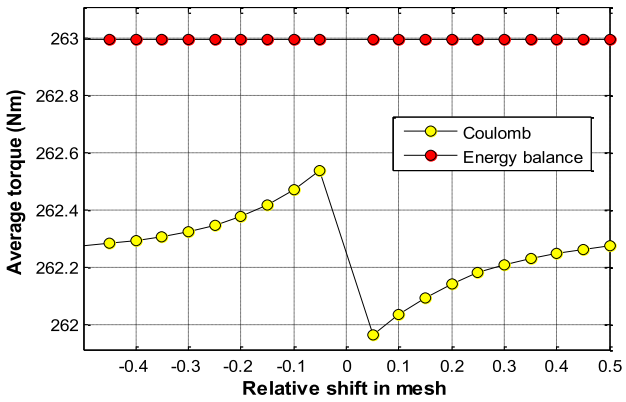

Fig. 12. Effect of the shape of the elements in average torques (nonlinear case and implicit Euler).

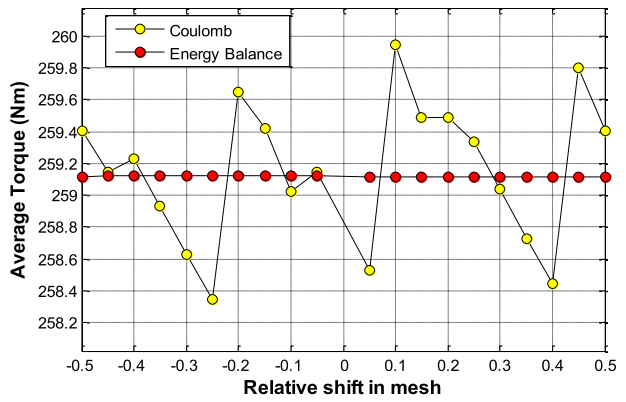

Fig. 13. Effect of the shape of elements in average torques when two layers of elements are used in the air gap.

were computed using discrete Fourier transform. The distortion d of the torque waveform was calculated from the dc component T_0 and other larger harmonics T_i

$$d = \frac{\sqrt{\sum T_i^2}}{T_o}. \tag{12}$$

This study was done for two different cases. In the first case, the same band of elements was used for both rotation and the torque computation, while in the second case different

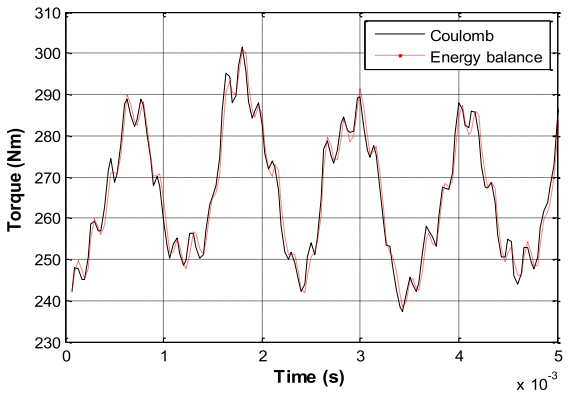

Fig. 14. Time variation of torque.

bands were used. In addition, each case was studied for a two layered mesh and a three layered mesh, which means that four different mesh combinations are studied. All the simulations in this case were done for a linear problem and the trapezoidal rule was used for all time integrations. Fig. 15 shows the distortion in torque with respect to the number of time steps per period used in the time-stepping simulation when calculated with Coulomb's method. The numbers in the legend is the mesh combination as shown in Table II, for instance, 2-2-1 means that the mesh used is a two layered mesh with second band used for rotation and first band used for the torque computation. It can be seen that the distortion is relatively higher when we use the same band of elements for both rotation and torque computation. This holds for both two layered and three layered mesh. The calculated distortion is slightly lower in the case when different bands of element are used for rotation and torque computation. What should be noted here is that the total harmonic distortion in torque computed by Coulomb's method is also dependent on the finite element mesh in the air gap. The energy balance method shows lower distortion in torque than other methods when the number of time steps per period is small, as shown in Fig. 16. This method requires smaller step size to accurately model the torque harmonics of the machine. The accuracy increases as the number of time steps per period increases. The choice of the band for rotation and torque computation did not affect the distortion. However, the results differ slightly for mesh with different number of layers of elements in the air gap. All the simulations were done for a full load slip.

V. Discussion

In the finite element analysis of induction machine, generally a mesh with two layers of elements are used in the air gap. This reduces the computation time, since the air gap of induction machine is narrow and descretizing it with three or more layers of elements will increase computation time and effort. However, use of three or more layers of elements ensures accuracy and therefore is recommended if the resources allow. The results of the study in this paper show that the numerical computation of the electromagnetic torque is dependent on the type of finite element mesh used for computation. The average torque computed from two methods

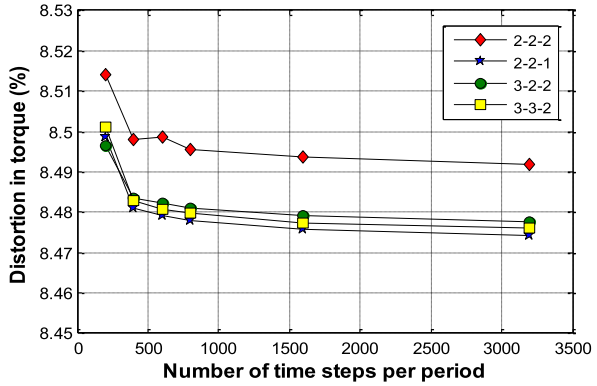

Fig. 15. Distortion of torque as a function of number of time step per period of 50 Hz supply frequency (Coulomb's method).

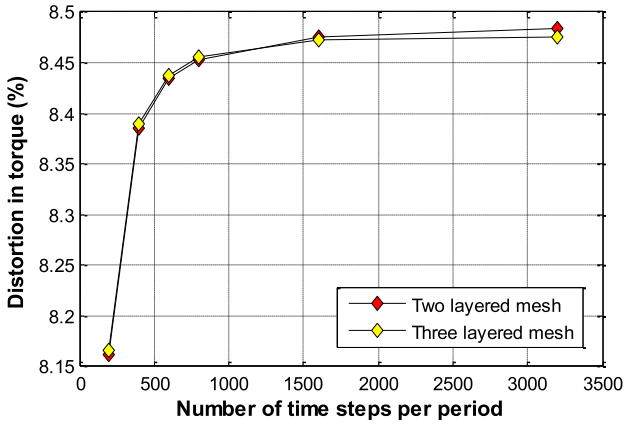

Fig. 16. Distortion of torque as a function of number of time step per period of 50 Hz supply frequency (energy balance).

Coulomb's method and the energy balance method are very close when the same band of elements are used for rotation and torque computation. The choice of the torque computation band did not affect the torque from the energy balance method, but the torque from Coulomb's method varied for different bands. The results also show that the torque is less sensitive to change in element shape in case of a three-layered mesh than the two-layered mesh. The shape of the elements used in the finite element simulation affects the torque if calculated from direct computation method. The above are true for both linear and nonlinear cases. Equilateral triangular elements gave best results. In addition, the torque when computed from the regular band of elements gives better results than that using irregular band of elements. The energy balance method seems to be insensitive to the change in the type of mesh used in the air gap and the shape of elements used in the torque computation band. This means that a relatively sparse finite element mesh can also result in an accurate torque computation when the energy balance method is used. This is very advantageous in terms of the computing resources and time needed. The time integration method used in the simulations, however, affects the torque calculated from the energy balance method. For instance, in the results shown in Figs. 11 and 12 when implicit Euler was used for time integration, if an average

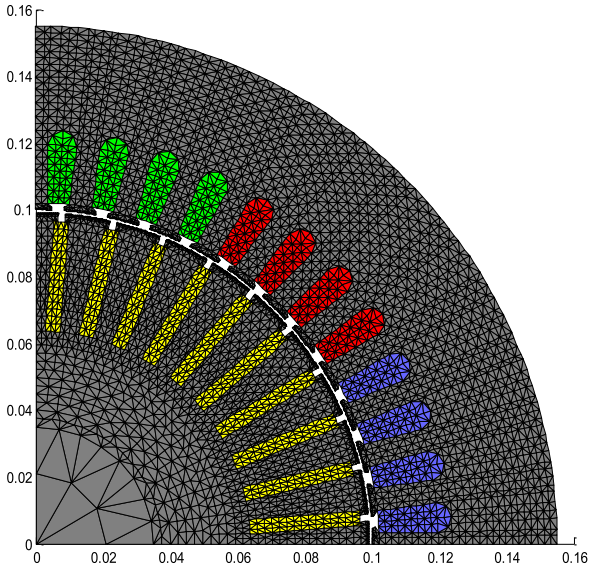

Fig. 17. Fine mesh in a quarter of the machine cross section.

of the average torques obtained from the Coulomb's methods for all element shapes is calculated, the result is not very close to the average torque from energy balance as it is in the case when the trapezoidal rule is used, for example, in Figs. 9 and 10. This is probably because the error in the energy balance for the implicit Euler method was significantly higher than the error for the trapezoidal rule. The energy balance is good when the trapezoidal rule is used, therefore, the difference between the torque from energy balance method and the Coulomb's method is quite small even when the number of time step is reduced. But this is not the case when the implicit Euler is used. For instance, if 200 time steps per period is used in the simulation, the difference is 0.2283 Nm for the trapezoidal rule and 2.3859 Nm for implicit Euler.

It has also been seen that the total harmonic distortion in the torque is also dependent on the type of mesh used in the air gap. When computed with the Coulomb's method, the torque seems to have more distortion if the torque is computed from the same band that is used for rotation. The torque may have slightly higher ripples. This is because when the mesh is changed at every time step, the corresponding element matrix is not continuous, which may causes jump in the torque. This can, however, be minimized using finer elements.

The effect of the mesh in the air gap of the machine is the prime interest in this paper. Now, the important question is if the torque computation is affected only by the finite element discretization in the air gap of the machine or also due to that of the whole problem area. To answer this question, the machine cross section was discretized with a fine mesh consisting of 13 228 elements and 27 701 nodes, as shown in Fig. 17. The main idea was to see if there was any change in the torque computed by both the methods used and if yes, how much. To get more reference, the fine mesh was refined to get an extra fine mesh with 15 556 elements and 31 361 nodes. A time-stepping finite element simulation was performed with 600 time steps per period of supply frequency and three

TABLE III
AVERAGE TORQUES COMPUTED FOR NORMAL MESH, FINE MESH, AND EXTRA FINE MESH

		Normal Mesh		Fine Mesh		Extra Fine Mesh	
		Linear	Non-Linear	Linear	Non-Linear	Linear	Non-Linear
Trapezoidal Rule	Torque (Coulomb)	259.5006	262.6781	259.2252	262.4273	259.0227	262.2843
	Torque (Energy balance)	259.1195	262.3375	259.0866	262.3079	259.0363	262.3008
	Diff. between CO & EB	0.3811	0.3406	0.1386	0.1194	0.0136	0.0165
Implicit Euler	Torque (Coulomb)	259.4476	262.6179	259.1334	262.3664	258.9698	262.2234
	Torque (Energy balance)	259.8337	262.9974	259.7616	262.9638	259.7500	262.9566
	Diff. between CO & EB	0.3861	0.3795	0.6282	0.5974	0.7802	0.7332

periods were simulated. The comparison of the results from the normal mesh, fine mesh, and extra fine mesh are shown in Table III. Both the fine and extra fine mesh were simulated for a linear and non-linear case using both the time-integration rules.

From the results it is clear that when trapezoidal rule is used, for the fine mesh the difference between the torque from Coulomb's method and energy balance method decreases and for the extra fine mesh, these two torques are even more close. But the result is opposite when the implicit Euler is used. In this case, the difference increases with mesh refinement. These results suggest that when the energy is conserved, that is for the trapezoidal rule both Coulomb's method and energy balance give same torque if the effect of the meshing is minimized but for implicit Euler it is not true. It is also seen in Table III that the torque from energy balance is less sensitive to the meshing. For instance, if we consider the non-linear case the torque from the energy balance with extra fine mesh differ by 0.0367 by that with a normal mesh, while the torque from Coulomb's method differ by 0.3938.

The torques obtained from the numerical torque computation methods were also compared with that obtained from the actual measurement. For this purpose, torques of three induction machines with different power ratings was measured. Each machine was simulated at the same operating point as in the measurements and the average torque was calculated using two-layered mesh in the air gap. The results from the measurements and the simulation are shown in Table IV. Torques from both the numerical methods show a quite good agreement with the measured results.

TABLE IV
COMPARISON WITH THE MEASUREMENT

Rated Power (kW)	Measured (Nm)	Coulomb's Torque (Nm)	Energy Balance Torque (Nm)
15	100.40	100.5822	100.2766
30	118.20	118.3106	118.1973
37	238.10	238.5136	238.1564

VI. CONCLUSION

This paper studies the torque computation in the numerical analysis of the electrical machine for different types of possible mesh combinations in the air gap of the machine. Coulomb's method of virtual work is used to compute torque and is compared with a method based on the energy balance of the machine. The effect of different types of mesh and the shape of the elements in torque computation is studied. The energy balance provides a reliable method for torque computation, but it can only be applied when the torque transmits a significant part of the input power. It is not valid for a locked rotor condition and may also have an accuracy problem at no load condition. It gives fairly good results if the time integration method has relatively lower order of error in the energy balance.

ACKNOWLEDGMENT

This work was supported by the Academy of Finland, Helsinki.

REFERENCES

[1] K. Reichert, H. Freundl, and W. Vogt, "The calculation of forces and torques within numerical magnetic field calculation methods," in *Proc. Comput. Electromagn. Fields (COMPUMAG)*, Oxford, U.K., Mar./Apr. 1976, pp. 64–73.

[2] J. L. Coulomb, "A methodology for the determination of global electromechanical quantities from a finite element analysis and its application to the evaluation of magnetic forces, torques and stiffness," *IEEE Trans. Magn.*, vol. 19, no. 6, pp. 2514–2519, Nov. 1983.

[3] A. Abdel-Razek, J. L. Coulomb, M. Feliachi, and J. C. Sabonnadiere, "Conception of an air-gap element for the dynamic analysis of the electromagnetic field in electric machines," *IEEE Trans. Magn.*, vol. 18, no. 2, pp. 655–659, Mar. 1982.

[4] A. Arkkio, "Analysis of induction motors based on the numerical solution of the magnetic field and circuit equations," Ph.D. dissertation, Lab. Electromech., Helsinki Univ. Technol., Espoo, Finland, Dec. 1987.

[5] N. Sadowski, Y. Lefevre, M. Lajoie-Mazenc, and J. Cros, "Finite element torque calculation in electrical machines while considering the movement," *IEEE Trans. Magn.*, vol. 28, no. 2, pp. 1410–1413, Mar. 1992.

[6] M. Marinescu and N. Marinescu, "Numerical computation of torques in permanent magnet motors by Maxwell stresses and energy method," *IEEE Trans. Magn.*, vol. 24, no. 1, pp. 463–466, Jan. 1988.

[7] D. G. Dorrell, M. Popescu, and M. I. McGilp, "Torque calculation in finite element solutions of electrical machines by consideration of stored energy," *IEEE Trans. Magn.*, vol. 42, no. 10, pp. 3431–3433, Oct. 2006.

[8] K. Hameyer, R. Mertens, U. Pahner, and R. Belmans, "New technique to enhance the accuracy of 2-D/3-D field quantities and forces obtained by standard finite-element solutions," *IEE Proc. Sci., Meas. Technol.*, vol. 145, no. 2, pp. 67–75, Mar. 1998.

[9] M. Popescu, D. M. Ionel, T. J. E. Miller, S. J. Dellinger, and M. I. McGilp, "Improved finite element computations of torque in brushless permanent magnet motors," *IEE Proc. Elect. Power Appl.*, vol. 152, no. 2, pp. 271–276, Mar. 2005.

[10] X. Wang and A. Qiu, "Calculation of cogging torque in squirrel-cage induction motors," in *Proc. Int. Conf. Elect. Mach. Syst. (ICEMS)*, Oct. 2010, pp. 1347–1350.

[11] S. T. Lee and L. M. Tolbert, "Analytical method of torque calculation for interior permanent magnet synchronous machines," in *Proc. IEEE Energy Convers. Congr. Exposit. (ECCE)*, Sep. 2009, pp. 173–177.

[12] D. Zarko, D. Ban, and T. A. Lipo, "Analytical solution for electromagnetic torque in surface permanent-magnet motors using conformal mapping," *IEEE Trans. Magn.*, vol. 45, no. 7, pp. 2943–2954, Jul. 2009.

[13] A. A. Abdel-Razek, J. L. Coulomb, M. Feliachi, and J. C. Sabonnadiere, "The calculation of electromagnetic torque in saturated electric machines within combined numerical and analytical solutions of the field equations," *IEEE Trans. Magn.*, vol. 17, no. 6, pp. 3250–3252, Nov. 1981.

[14] W. Rong-Jie and M. J. Kamper, "Force calculation of electric machines with a flat air-gap using hybrid finite element mesh," in *Proc. 19th Int. Conf. Elect. Mach. (ICEM)*, Sep. 2010, pp. 1–3.

[15] L. Yanni and D. C. Aliprantis, "Optimal design of electromechanical devices using a hybrid finite element/air-gap element method," in *Proc. IEEE Power Energy Conf. Illinois (PECI)*, Feb. 2013, pp. 106–113.

[16] N. Shuangxia, S. L. Ho, and W. N. Fu, "Power balanced electromagnetic torque computation in electric machines based on energy conservation in finite-element method," *IEEE Trans. Magn.*, vol. 49, no. 5, pp. 2385–2388, May 2013.

[17] P. Rasilo, L. Perkkio, A. Hannukainen, B. Silwal, T. Eirola, and A. Arkkio, "Instantaneous power balance in finite-element simulation of electrical machines," *IEEE Trans. Magn.*, vol. 50, no. 5, pp. 1–7, May 2014.

[18] E. Hairer, C. Lubich, and G. Wanner, "Geometric numerical integration," in *Structure-Preserving Algorithms for Ordinary Differential Equations*. Berlin, Germany: Springer-Verlag, 2002.

[19] B. Silwal, P. Rasilo, L. Perkkio, A. Hannukainen, T. Eirola, and A. Arkkio, "Evaluation and comparison of different numerical computation methods for the electromagnetic torque in electrical machines," in *Proc. Int. Conf. Elect. Mach. Syst. (ICEMS)*, Oct. 2013, pp. 837–842.